Study of one-dimensional nature of $S=1/2$ $(Sr,Ba)_2Cu(PO_4)_2$ and $BaCuP_2O_7$ via ^{31}P NMR

R. Nath and A. V. Mahajan
Department of Physics, Indian Institute of Technology, Mumbai 400076, India

N. Büttgen, C. Kegler, and A. Loidl
Experimentalphysik V, Elektronische Korrelationen und Magnetismus, Institut für Physik, Universität Augsburg, D-86135 Augsburg, Germany

J. Bobroff
Laboratoire de Physique des Solides, Universite Paris-Sud, 91405 Orsay, France
(Received 25 August 2004; revised manuscript received 7 February 2005; published 31 May 2005)

The magnetic behavior of the low-dimensional phosphates $(Sr,Ba)_2Cu(PO_4)_2$ and $BaCuP_2O_7$ was investigated by means of magnetic susceptibility and ^{31}P nuclear magnetic resonance (NMR) measurements. We present here the NMR shift, the spin-lattice $(1/T_1)$, and spin-spin $(1/T_2)$ relaxation-rate data over a wide temperature range $0.02\ K \leqslant T \leqslant 300\ K$. The temperature dependence of the NMR shift $K(T)$ is well described by the $S=1/2$ Heisenberg antiferromagnetic chain model [D. C. Johnston, R. K. Kremer, M. Troyer, X. Wang, A. Klümper, S. L. Bud'ko, A. F. Panchula, and P. C. Canfield, Phys. Rev. B **61**, 9558 (2000)] with an intrachain exchange of $J/k_B \simeq 165$, 151, and 108 K in $Sr_2Cu(PO_4)_2$, $Ba_2Cu(PO_4)_2$, and $BaCuP_2O_7$, respectively. Deviations from Johnston's expression are seen for all these compounds in the T dependence of $K(T)$ at low temperatures. ^{31}P is located symmetrically between the Cu ions and fluctuations of the staggered susceptibility at $q=\pi/a$ should be filtered out due to vanishing of the geometrical form factor. However, the qualitative temperature dependence of our ^{31}P NMR $1/T_1$ indicates that relaxation due to fluctuations around $q=\pi/a$ (but $\neq \pi/a$) have the same T dependence as those at $q=\pi/a$ and apparently dominate. Our measurements suggest the presence of magnetic ordering at 0.85 K in $BaCuP_2O_7$ ($J/k_B \simeq 108$ K) and a clear indication of a phase transition (divergence) in $1/T_1(T)$, $1/T_2(T)$, and a change of the line shape is observed. This enables us to investigate the one-dimensional (1D) behavior over a wide temperature range. We find that $1/T_1$ is nearly T independent at low temperatures ($1\ K \leqslant T \leqslant 10\ K$), which is theoretically expected for 1D chains when relaxation is dominated by fluctuations of the staggered susceptibility. At high temperatures, $1/T_1$ varies nearly linearly with temperature, which accounts for contribution of the uniform susceptibility.

DOI: 10.1103/PhysRevB.71.174436 PACS number(s): 75.10.Pq, 75.40.Cx, 76.60.−k, 76.60.Cq

I. INTRODUCTION

There is presently a lot of interest in the magnetic properties of one-dimensional (1D) Heisenberg antiferromagnetic (HAF) spin systems. This is because of the rich physics that they exhibit, in addition to the fact that such systems are tractable from a computational and theoretical standpoint. In particular, qualitative differences are expected between integer-spin and half-integer-spin HAF chains. Although the integer-spin chains are gapped,[1] the half-integer-spin chains are said to have quasi-long-range order (LRO) because of the gradual spatial decay (power-law) of the spin-spin correlation function.[2,3]

The magnetic Hamiltonian describing a spin-half Heisenberg chain can be written as $H=-J\Sigma_i S_i \cdot S_{i+1}$, where J is the intrachain coupling constant between the nearest-neighbor spins. The temperature dependence of the magnetic susceptibility $\chi(T)$ for the $S=1/2$ HAF chain was numerically calculated by Bonner and Fisher,[4] and since then, the Bonner-Fisher expression has been used by experimentalists to determine the value of the exchange coupling (J) from the temperature dependence of the bulk susceptibility. A more accurate and analytical evaluation of the susceptibility of $S=1/2$ HAF chain was done by Eggert *et al.*[5] which is valid at low-temperatures. Via numerical simulations, an expression for $\chi(T)$ accurate for both low and high temperatures ($5\times10^{-25} \leqslant k_BT/J \leqslant 5$, with k_B the Boltzmann constant) was given by Johnston *et al.*[6] Dynamical properties of $S=1/2$ chains have also been theoretically investigated. In particular, work has been focused on the properties measured by nuclear magnetic resonance (NMR) techniques. Sachdev[7] determined the temperature dependence of the NMR spin-lattice $(1/T_1)$ and the Gaussian spin-spin $(1/T_{2G})$ relaxation rates for half-integer spin chains for $k_BT/J \ll 1$ as $1/T_1 = \text{constant}$ and $1/T_{2G} \propto 1/\sqrt{T}$. Quantum Monte Carlo calculations by Sandvik[8] support these results over an appropriate temperature range. These results are at variance from those for classical spin chains $S=\infty$, where theory predicts[9] $1/T_1$ and $1/T_{2G} \propto T^{-3/2}$.

Although the one-dimensional (1D) compounds $CuCl_2 \cdot 2NC_5H_5$ and $KCuF_3$ have been experimentally investigated previously,[10,11] the onset of LRO (at the ordering temperature T_N) due to interchain interactions prevents the study of true 1D properties down to low temperatures. For the abovementioned 1D compounds, the ratios $k_BT_N/J \simeq 0.084$ and 0.1195, respectively, have been determined. Dynamic and static properties of Sr_2CuO_3 1D chain have been extensively studied.[12–16] Because of the large value of J/k_B

($\approx$2200 K) and the very weak interchain couplings, this compound orders only below 5 K and hence 1D properties could be studied in a large range of temperature. However, precisely because of this large value of J/k_B in Sr_2CuO_3, the NMR work was limited to the low-temperature region, i.e., $k_BT/J \lesssim 0.15$. It is clearly useful to examine different compounds that might exhibit 1D behavior in a large temperature range, thereby allowing for a comparison with theoretical models and improving our understanding of such systems.

$Sr_2Cu(PO_4)_2$ (Ref. 17) and $Ba_2Cu(PO_4)_2$ (Ref. 18) are two isostructural compounds having a monoclinic unit cell with space group $C_{2/m}$. The reported lattice constants are $a=11.515$ Å, $b=5.075$ Å, $c=6.574$ Å and $a=12.160$ Å, $b=5.133$ Å, $c=6.885$ Å for $Sr_2Cu(PO_4)_2$ and $Ba_2Cu(PO_4)_2$, respectively. $BaCuP_2O_7$, which differs slightly in structure compared to the other two, crystallizes in a triclinic unit cell with space group $P\bar{1}$ and lattice constants $a=7.353$ Å, $b=7.578$ Å, and $c=5.231$ Å.[19] In the former two compounds, each CuO_4 square plane shares its edges with two similar kinds of PO_4 groups. The edge sharing takes place in one direction, forming an isolated $[Cu(PO_4)_2]_\infty$ chain along the crystallographic b direction. A likely interaction path of Cu^{2+} ions is sketched in Fig. 1(a). As opposed to $Sr_2Cu(PO_4)_2$ and $Ba_2Cu(PO_4)_2$, $BaCuP_2O_7$ contains two inequivalent ^{31}P atoms, where each CuO_4 plaquette shares its edges with two different PO_4 groups forming chains as shown in Fig. 1(b). Unlike the isolated chains of $Sr_2Cu(PO_4)_2$ and $Ba_2Cu(PO_4)_2$, there appear to be pairs of chains in $BaCuP_2O_7$. Only Etheredge and Hwu[18] have published the bulk susceptibility as a function of temperature for $Ba_2Cu(PO_4)_2$. However, the authors failed to comment on the broad maximum at 80 K presumably because it was suppressed by a high Curie contribution present in their sample.

In this paper we present, in detail, the magnetic properties of the 1D copper phosphates, $Sr_2Cu(PO_4)_2$, $Ba_2Cu(PO_4)_2$, and $BaCuP_2O_7$ using ^{31}P NMR as a local probe. NMR is regarded as a valuable tool for the study of microscopic properties of 1D chains, especially through the studies of the NMR shift (K), the spin-spin relaxation rate ($1/T_2$), and the spin-lattice relaxation rate ($1/T_1$). We report on measurements of the bulk susceptibility $\chi(T)$ for 1.8 K $\leqslant T \leqslant$ 400 K and $K(T)$, $1/T_1(T)$, and $1/T_2(T)$ of ^{31}P NMR in a large temperature range (0.02 K $\leqslant T \leqslant$ 300 K). This range not only covers temperatures well below J/k_B but also up to $\sim 1.5J/k_B$ for $Sr_2Cu(PO_4)_2$ and $Ba_2Cu(PO_4)_2$, and up to $T \sim 3J/k_B$ for $BaCuP_2O_7$. The experimental details concerning sample preparation and various measurements are given in Sec. II. Section III contains our experimental results, and a detailed discussion about the results is presented in Sec. IV. Our work on these compounds strongly suggests that they are some of the best examples of $S=1/2$ 1D HAF systems. In the course of our work, magnetic susceptibility and heat capacity of $Sr_2Cu(PO_4)_2$, $Ba_2Cu(PO_4)_2$, and $BaCuP_2O_7$ were reported by Belik *et al.*[20,21] They found the exchange constant (J/k_B) to be 144 K for $Sr_2Cu(PO_4)_2$, 132 K for $Ba_2Cu(PO_4)_2$, and 103.6 K for $BaCuP_2O_7$. Presence of any LRO was not seen from specific heat measurement down to 0.45 K for $Sr_2Cu(PO_4)_2$ and $Ba_2Cu(PO_4)_2$, whereas $BaCuP_2O_7$ showed ordering at 0.81 K.

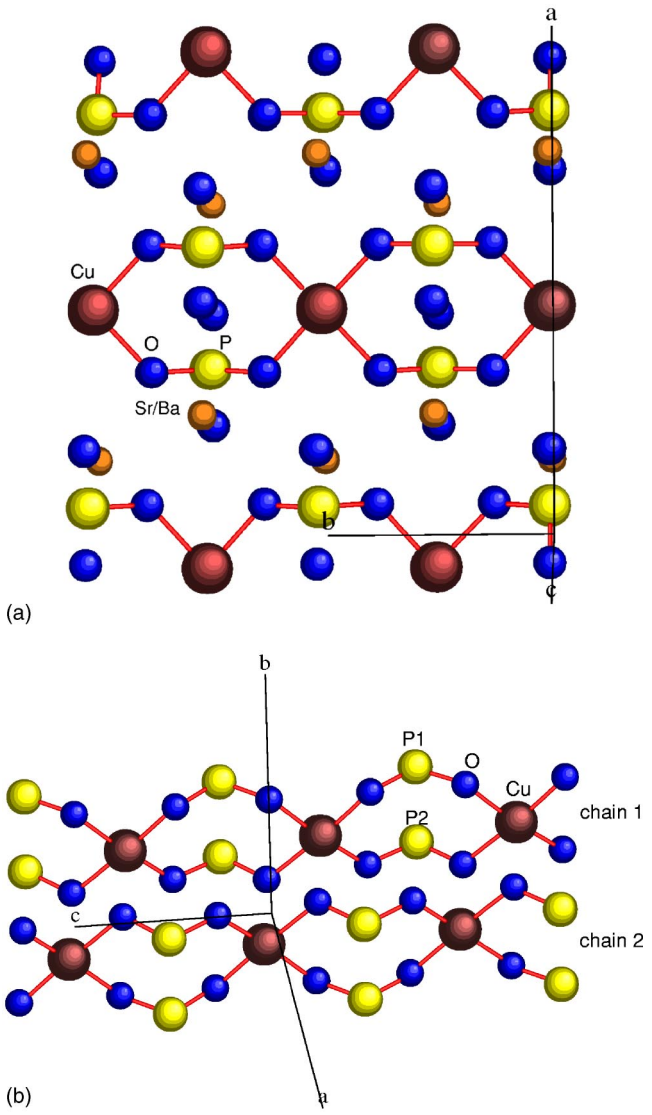

FIG. 1. Schematic diagram of $[Cu(PO_4)_2]_\infty$ linear chains (a) propagating along b direction for $(Ba/Sr)_2Cu(PO_4)_2$ and (b) along the c direction for $BaCuP_2O_7$. The possible interaction paths are shown by solid lines between atoms.

II. EXPERIMENTAL DETAILS

Polycrystalline samples of $Sr_2Cu(PO_4)_2$, $Ba_2Cu(PO_4)_2$, and $BaCuP_2O_7$ were prepared by solid-state reaction techniques using $BaCO_3$ (99.9% pure), $SrCO_3$ (99.999% pure), CuO (99.99% pure), and $(NH_4)_2HPO_4$ (99.9% pure) as starting materials. The stoichiometric mixtures were fired at 800 C ($Sr_2Cu(PO_4)_2$), 700 C ($Ba_2Cu(PO_4)_2$), and 650 C ($BaCuP_2O_7$) for 120 h each, in air, with several intermediate grindings and pelletization. Finally some amounts of each of the samples were annealed at 400 C under a reducing atmosphere (5% H_2 in Ar) in an attempt to reduce the Curie contribution in the bulk susceptibility. Nearly single phases were confirmed from x-ray diffraction, which was performed with a Philips Xpert-Pro powder diffractometer. A Cu target was used in the diffractometer with $\lambda_{av}=1.541\,82$ Å. Lattice parameters were calculated using a least-squares fit procedure.

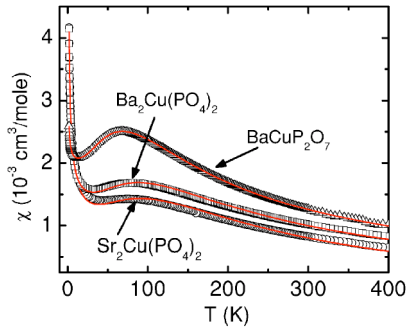

FIG. 2. Magnetic susceptibility (M/H) vs temperature T for $Sr_2Cu(PO_4)_2$, $Ba_2Cu(PO_4)_2$, and $BaCuP_2O_7$ in an applied field of 5 kG. The solid lines are best fits of the data to Eq. (1).

The obtained lattice constants are [$a=11.496(5)$ Å, $b=5.069(2)$ Å, $c=6.566(3)$ Å], [$a=12.138(2)$ Å, $b=5.123(1)$ Å, $c=6.868(1)$ Å] and [$a=7.338(2)$ Å, $b=7.561(2)$ Å, $c=5.217(1)$ Å] for $Sr_2Cu(PO_4)_2$, $Ba_2Cu(PO_4)_2$, and $BaCuP_2O_7$, respectively. These are in agreement with previously reported values.[17–19]

Magnetization (M) data were measured as a function of temperature T ($1.8\ \mathrm{K} \leqslant T \leqslant 400\ \mathrm{K}$) and applied field H ($0 \leqslant H \leqslant 50$ kG) using a superconducting quantum interference device (SQUID) magnetometer.

The NMR measurements were carried out using pulsed NMR techniques on ^{31}P nuclei (nuclear spin $I=1/2$ and gyromagnetic ratio $\gamma/(2\pi)=17.237$ MHz/T) in a large temperature range ($0.02\ \mathrm{K} \leqslant T \leqslant 300\ \mathrm{K}$). We have done the measurements at two different applied fields of about 55 kG and 4 kG, which correspond to radio frequencies (rf) of about 95 MHz and 6.8 MHz, respectively.

For $2\ \mathrm{K} \leqslant T \leqslant 300\ \mathrm{K}$, NMR measurements were done in a 55 kG applied field with a ^{4}He cryostat (Oxford Instruments). Spectra were obtained by Fourier transform (FT) of the NMR echo signals using a $\pi/2$ pulse of width of about 4 μs. The NMR shift $K(T)=[\nu(T)-\nu_{\mathrm{ref}}]/\nu_{\mathrm{ref}}$ was determined by measuring the resonance frequency of the sample [$\nu(T)$] with respect to a standard H_3PO_4 solution (resonance frequency ν_{ref}). The spin-lattice relaxation rate ($1/T_1$) was determined by the inversion-recovery method. The spin-spin relaxation rate ($1/T_2$) was obtained by measuring the decay of the echo integral with variable spacing between the $\pi/2$ and the π pulse.

In the $0.02\ \mathrm{K} \leqslant T \leqslant 10\ \mathrm{K}$ range, NMR measurements were performed using a ^{3}He/^{4}He dilution refrigerator (Oxford Instruments) with the resonant circuit inside the mixing chamber. Spectra were obtained by field sweeps at a constant radio frequency (ν_{rf}) of 95 MHz. $1/T_1$ was measured down to 0.02 K following the same procedure as described above using $\pi/2$ pulse of width 15 μs. Lower rf power (and consequently longer pulse widths) were used to avoid rf heating of the sample. Measurements were also done in a low-field of about 4 kG ($\nu_{\mathrm{rf}} \simeq 6.8$ MHz), where the NMR line was narrow and inversion of the nuclear magnetization by a π pulse of width 30 μs was assured. The data from low-field measurements almost reproduce the high-field data.

III. RESULTS

A. Bulk susceptibility

Magnetic susceptibilities $\chi(T)$ ($=M/H$) for all the three compounds were measured as a function of temperature in an applied field of 5 kG (Fig. 2). The amount of ferromagnetic impurities present in our samples were estimated from the intercept of M versus H isotherms at various temperatures and were found to be 19, 12, and 30 ppm of ferromagnetic Fe^{3+} ions for $Sr_2Cu(PO_4)_2$, $Ba_2Cu(PO_4)_2$, and $BaCuP_2O_7$, respectively. The data in Fig. 2 have been corrected for these ferromagnetic impurities. As shown in the figure, all the samples exhibit a broad maximum, indicative of low-dimensional magnetic interactions. With decrease in temperature, susceptibility increases in a Curie-Weiss manner. This possibly comes from chain ends, natural defects, excess oxygen, and extrinsic paramagnetic impurities present in the samples. No obvious features associated with LRO are seen for $1.8\ \mathrm{K} \leqslant T \leqslant 400\ \mathrm{K}$ for any of the samples. A substantial reduction of Curie terms was achieved by annealing the samples at 400 °C in an atmosphere of 5% H_2 in Ar. Similar experiments in Sr_2CuO_3 and $YBaNiO_5$ lead to reduced Curie terms.[22,23] The data in Fig. 2 pertain to $Sr_2Cu(PO_4)_2$ and $Ba_2Cu(PO_4)_2$, annealed in a reducing atmosphere. Since the Curie contribution in the case of as-prepared $BaCuP_2O_7$ is not large, we did not treat this sample in a reducing atmosphere.

In order to fit the bulk susceptibility data, we assume that the susceptibility consists of three terms

$$\chi = \chi_0 + \frac{C}{T+\theta} + \chi_{\mathrm{spin}}(T), \tag{1}$$

where $\chi_{\mathrm{spin}}(T)$ is the uniform spin susceptibility for a $S=1/2$ 1D HAF system given in Ref. 6 (expression corresponding to "fit2"). This expression (containing the Landé g factor and J as fitting parameters) is not reproduced here because it is somewhat unwieldy. The first term χ_0 is temperature independent and consists of diamagnetism of the

TABLE I. Values of the parameters (χ_0, C, θ, and J/k_B) obtained by fitting the bulk susceptibility to Eq. (1) for each of the three samples.

Sample	χ_0 10^{-3} cm^3/mole	C 10^{-3} cm^3 K/mole	θ K	J/k_B K
$Sr_2Cu(PO_4)_2$	0.005±0.001	10.6±0.6	1.1	152±12
$Ba_2Cu(PO_4)_2$	−0.15±0.02	6.8±0.25	0.5	146±10
$BaCuP_2O_7$	−0.07±0.005	1.6±0.06	0.4	108±3

core electron shells (χ_{core}) and Van-Vleck paramagnetism (χ_{vv}) of the open shells of the Cu^{2+} ions present in the sample. The second term $C/(T+\theta)$ is the Curie-Weiss contribution due to paramagnetic species in the sample.

The average Landé g-factors determined from an analysis of the powder spectra from electron paramagnetic resonance (EPR) experiments on our samples were found to be 2.15, 2.15, and 2.2 for $Sr_2Cu(PO_4)_2$, $Ba_2Cu(PO_4)_2$, and $BaCuP_2O_7$, respectively. Our experimental $\chi(T)$ data were fitted using the above g values (the solid lines are the best fits in Fig. 2) and the extracted parameters are listed in Table I.

Adding the core diamagnetic susceptibility for the individual ions,[24] the total χ_{core} was calculated to be -1.39×10^{-4} cm^3/mole, -1.73×10^{-4} cm^3/mole, and -1.29×10^{-4} cm^3/mole for $Sr_2Cu(PO_4)_2$, $Ba_2Cu(PO_4)_2$, and $BaCuP_2O_7$, respectively. The Van-Vleck paramagnetic susceptibility for our samples estimated by subtracting χ_{core} from χ_0 gives $\chi_{vv}=14.4\times10^{-5}$ cm^3/mole, 2.3×10^{-5} cm^3/mole, and 5.9×10^{-5} cm^3/mole for $Sr_2Cu(PO_4)_2$, $Ba_2Cu(PO_4)_2$, and $BaCuP_2O_7$, respectively. These values are comparable to that found in Sr_2CuO_3.[12] The Curie contributions present in the samples correspond to a defect spin concentration of 3, 1.8, and 0.4 % for $Sr_2Cu(PO_4)_2$, $Ba_2Cu(PO_4)_2$, and $BaCuP_2O_7$, respectively assuming defect spin $S=1/2$.

B. ^{31}P NMR

1. NMR shift

NMR has an important advantage over bulk susceptibility for the determination of magnetic parameters. Although the presence of a Curie-like contribution restricts the accurate determination of $\chi_{\text{spin}}(T)$ and hence J from $\chi(T)$, in NMR this paramagnetism broadens the NMR line but does not contribute to the NMR shift K. Therefore, it is more reliable to extract the $\chi_{\text{spin}}(T)$ and J from the temperature dependence of the NMR shift rather than from the bulk susceptibility. From Fig. 1 it appears that in all the compounds each ^{31}P is coupled to two Cu^{2+} ions via a supertransferred hyperfine interaction mediated by oxygen ions in its neighborhood. All the NMR data reported in this paper correspond to samples of $Sr_2Cu(PO_4)_2$ and $Ba_2Cu(PO_4)_2$, which were treated in a reducing atmosphere as described in Sec. II, while the data for $BaCuP_2O_7$ correspond to the as-prepared sample. We note here that we also did NMR measurements on the as-prepared $Sr_2Cu(PO_4)_2$ and $Ba_2Cu(PO_4)_2$ samples (for $T>10$ K) and found no differences with respect to the samples that were treated in a reducing atmosphere.

NMR shift data as a function of temperature are shown in Fig. 3. The samples exhibit broad maxima at different temperatures: $\approx$100 K for $Sr_2Cu(PO_4)_2$, $\approx$90 K for $Ba_2Cu(PO_4)_2$, and $\approx$70 K for $BaCuP_2O_7$, indicative of short-range ordering. Toward lower temperatures $T<20$ K, the NMR shift $K(T)$ shows a plateau as is demonstrated by the semilogarithmic plot in the inset of Fig. 3. In the sub-Kelvin region, the NMR shift $K(T)$ of all our samples decreases steeply. The falloff appears below $k_BT/J\simeq0.003$ for $Sr_2Cu(PO_4)_2$, $k_BT/J\simeq0.0033$ for $Ba_2Cu(PO_4)_2$, and $k_BT/J\simeq0.01$ for $BaCuP_2O_7$.

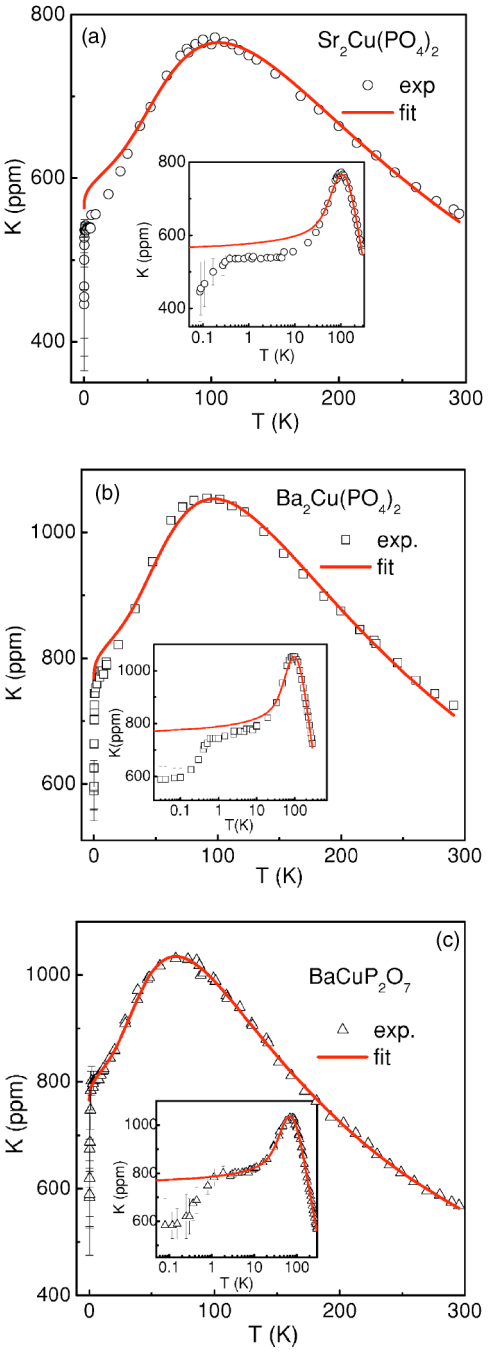

FIG. 3. ^{31}P shift K vs temperature T for (a) $Sr_2Cu(PO_4)_2$, (b) $Ba_2Cu(PO_4)_2$, and (c) $BaCuP_2O_7$. The solid lines are fits of Eq. (2) in the temperature range, 10 K$\leqslant T\leqslant$300 K and then extrapolated down to 0.01 K. Inset shows K vs T on a logarithmic temperature scale for improved visualisation of the low-T data.

The conventional scheme of analysis is to first determine the spin susceptibility (as done in the previous section) and then plot K versus χ_{spin} with T as an implicit parameter. The exchange coupling J is obtained from the susceptibility analysis, while the slope of the K versus χ_{spin} plot yields the total hyperfine coupling A between the ^{31}P nucleus and the two nearest-neighbor Cu^{2+} ions. As an example, such a $K-\chi_{\text{spin}}$ plot is shown in Fig. 4 for $BaCuP_2O_7$.

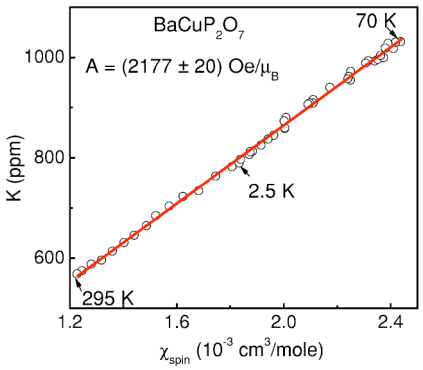

FIG. 4. ^{31}P shift K vs spin susceptibility χ_{spin} for $BaCuP_2O_7$. The solid line shows the linear fit.

Since an algebraic expression for the temperature dependence of the spin susceptibility (and therefore the spin-shift) is known in this case, we prefer to determine J and A simultaneously by fitting the temperature dependence of K to the following equation:

$$K = K_0 + \left(\frac{A}{N_A \mu_B}\right)\chi_{\text{spin}}(T,J) \qquad (2)$$

where K_0 is the chemical shift and N_A is the Avogadro number. While fitting, g was kept fixed to the value obtained from EPR analysis and K_0, A, and J were free parameters. The parameters J and A determined in this manner are considered more reliable, since the only temperature dependent term in the NMR shift is due to spin-susceptibility, whereas bulk susceptibility analysis is somewhat hampered by low-temperature Curie terms. As shown in Fig. 3, the shift data fit nicely to Eq. (2) in the temperature range $10\ \text{K} \leqslant T \leqslant 300\ \text{K}$ yielding the parameters given in Table II.

TABLE II. Values of the parameters (K_0, A, and J/k_B) obtained by fitting the NMR shift data to Eq. (2) in the temperature range $10\ \text{K} \leqslant T \leqslant 300\ \text{K}$ for each of the three samples.

Sample	K_0 ppm	A O_e/μ_B	J/k_B K
$Sr_2Cu(PO_4)_2$	47±17	2609±100	165±10
$Ba_2Cu(PO_4)_2$	40±15	3364±130	151±6
$BaCuP_2O_7$	73±20	2182±20	108±2

2. Spectra

For all the three compounds the ^{31}P NMR spectra consist of a single spectral line as is expected for $I=1/2$ nuclei (Fig. 5). As shown in the crystal structures in Fig. 1, $Sr_2Cu(PO_4)_2$ and $Ba_2Cu(PO_4)_2$ have a unique ^{31}P site, whereas in $BaCuP_2O_7$ there are two inequivalent ^{31}P sites. However, a single resonance line even for $BaCuP_2O_7$ implies that both the ^{31}P sites in this compound are nearly identical. Since our measurements are on randomly oriented polycrystalline samples, asymmetric shape of the spectra corresponds to a powder pattern due to an asymmetric hyperfine coupling constant and an anisotropic susceptibility. The linewidth was found to be field and temperature dependent as is shown in the insets of Figs. 5(a) and 5(b) for $(Sr/Ba)_2Cu(PO_4)_2$ and in Figs. 5(c) and 5(d) for $BaCuP_2O_7$, respectively. Although we did not do a detailed analysis of the linewidth, its T and H dependence is likely because of macroscopic field inhomogeneities due to the demagnetization effects of a powder sample[25] and paramagnetic impurities.

As seen from Fig. 5(c) the NMR spectra of $BaCuP_2O_7$ broaden abruptly below ~0.85 K. We then measured the spectral line shape in a low field ($H \simeq 4$ kG) below 0.85 K in

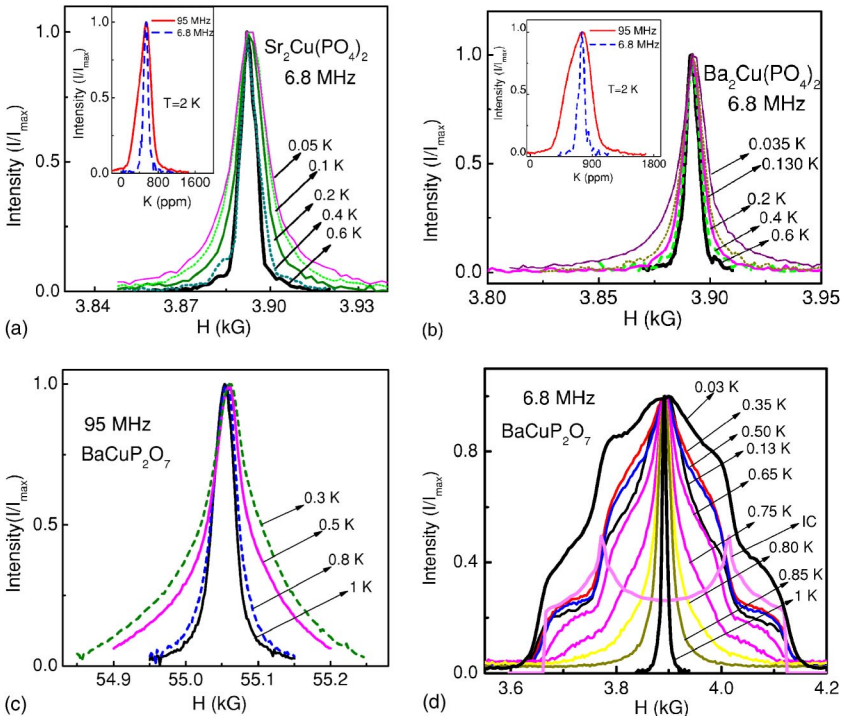

FIG. 5. Low-field ($H \simeq 4$ kG) ^{31}P NMR spectra at different temperatures T for (a) $Sr_2Cu(PO_4)_2$ and (b) $Ba_2Cu(PO_4)_2$. The insets of (a) and (b) contain the high-field and low-field spectra at 1 K. (c) and (d) show high-field and low-field spectra, respectively, for $BaCuP_2O_7$ at various temperatures below 1 K, showing the sudden change in line width. Also shown in (d) is the spectrum in case of IC order using Eq. (6) and parameters given in the text.

order to check whether any features could be resolved. Fig. 5(d) shows the appearance of two shoulders on either side of the central line below about 0.85 K. This is most likely an indication of the appearance of LRO. The positions of the shoulders stay unchanged with temperature, while their relative intensities increase with decreasing temperature. A more detailed discussion is carried out in Sec. IV.

3. Spin-lattice relaxation rate $1/T_1$

Temperature dependencies of ^{31}P $1/T_1$ are presented in Fig. 6. For the $1/T_1$ experiment, the central positions of corresponding spectra at high (55 kG) and low (4 kG) external fields have been irradiated. Inset of Fig. 6(a) shows the typical magnetization recovery at $H \simeq 55$ kG and at two different temperatures. For a spin-1/2 nucleus the recovery is expected to follow a single exponential behavior. In $Sr_2Cu(PO_4)_2$ and $Ba_2Cu(PO_4)_2$ (for $H \simeq 55$ kG), the recovery of the nuclear magnetization after an inverting pulse was single exponential down to 2 K, whereas for $T < 2$ K, it fitted well to the double exponential,

$$\frac{1}{2}\left(\frac{M(\infty)-M(t)}{M(\infty)}\right) = A_1 \exp\left(-\frac{t}{T_{1L}}\right) + A_2 \exp\left(-\frac{t}{T_{1S}}\right) + C, \tag{3}$$

where $1/T_{1L}$ corresponds to the slower rate and $1/T_{1S}$ is the faster component. $M(t)$ is the nuclear magnetization a time t after an inverting pulse. Since the deviation from single exponential behavior could be due to the large linewidth and our consequent inability to saturate the NMR line, we also performed experiments at a lower field ($\simeq$4 kG), where the line is about three times narrower [see insets of Fig. 5(a) or 5(b)]. However, even in low-field (where the rf field H_1 was sufficient to ensure complete inversion) the nuclear magnetization recovery is not single exponential, implying that this is an intrinsic effect. With increasing temperature, the ratio A_2/A_1 decreases and the recovery becomes single exponential for $T > 2$ K. It appears that the longer T_1 component comes from the chain itself, whereas the faster component is associated with ^{31}P nuclei near chain ends. Clearly, at lower temperatures, the chain-end-induced magnetization extends to large distances from chain ends (thereby affecting more ^{31}P nuclei) and, consequently, the weight associated with the faster relaxation is more at lower temperatures. From the experiment, it was found that low-field measurements reproduce almost the same T_1 as for high field.[26] Although we have measured T_1 down to 0.02 K, since the magnetization recovery is not single exponential, reliable relaxation rates $1/T_1$ could not be obtained below 0.1 K (where the faster component $1/T_{1s}$ has a large weight). Figures 6(a) and 6(b) display data down to 0.1 K, where it is seen that $1/T_1$ for $Sr_2Cu(PO_4)_2$ and $Ba_2Cu(PO_4)_2$ do not show any anomaly. Even at lower temperatures, there was no indication of a divergence of the relaxation rate, indicating the absence of any magnetic ordering. For 1 K $\leqslant T \leqslant$ 10 K, $1/T_1$ remains constant with temperature and below 0.5 K a slight increase was observed for both $Sr_2Cu(PO_4)_2$ and $Ba_2Cu(PO_4)_2$. At high temperatures ($T \geqslant 30$ K), $1/T_1$ varies nearly linearly with temperature.

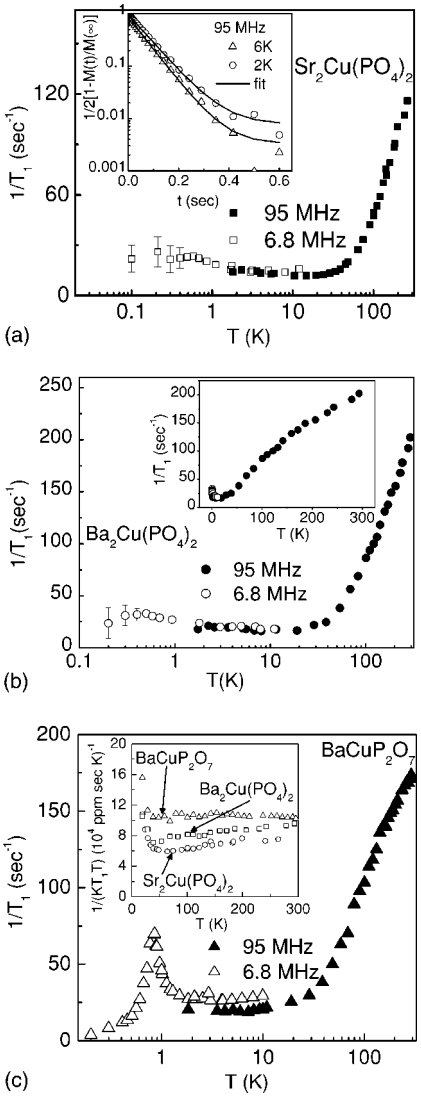

FIG. 6. Spin-lattice relaxation rate $1/T_1$ (both high and low fields) vs temperature T for (a) $Sr_2Cu(PO_4)_2$, (b) $Ba_2Cu(PO_4)_2$, and (c) $BaCuP_2O_7$. In the inset of (a), the normalized nuclear magnetization at high field is plotted as a function of pulse separation t (at 6 and 2 K) and the solid line is a single-exponential fit for $Sr_2Cu(PO_4)_2$. The inset of (b) displays the relaxation rate data for $Ba_2Cu(PO_4)_2$ on a linear temperature scale. In the inset of (c), the temperature dependence of $1/(KT_1T)$ is presented for the three compounds.

In $BaCuP_2O_7$, $1/T_1$ at $H \simeq 55$ kG was measured down to 3 K. Once again, the large linewidth prevented us from saturating the nuclear magnetization below 3 K. Low-field measurements give perfect single exponential recovery down to 2 K, and below 2 K it was fitted well to double exponential. From Fig. 6(c), it is clear that the $1/T_1(T)$ has a sharp peak at $T \approx 0.85$ K, indicating an approach to magnetic ordering. For 1 K $\leqslant T \leqslant$ 10 K, $1/T_1$ remains constant and for $T \geqslant 15$ K, it varies linearly with temperature. A slight change in magnitude in low-field data compared to high-field data may be due to spin-diffusion.[13]

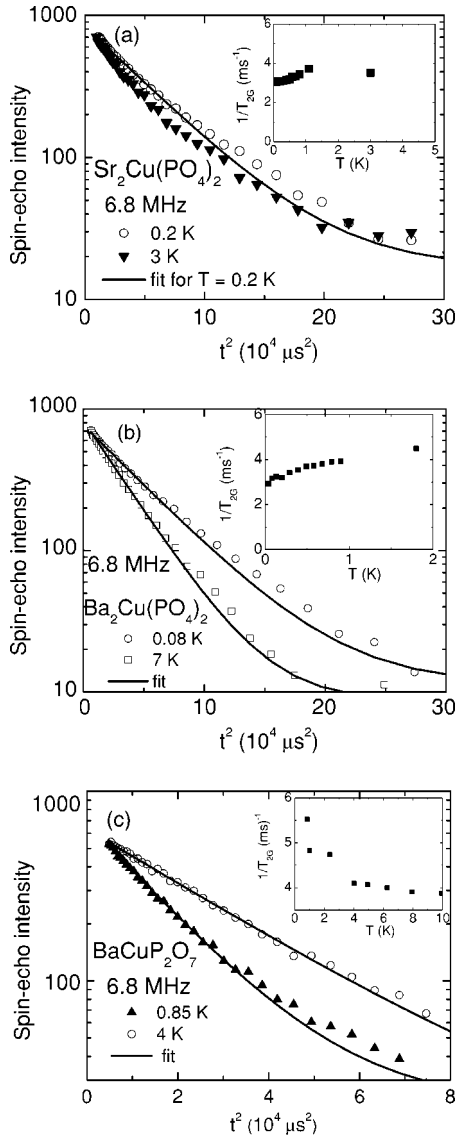

FIG. 7. Spin-echo decays are plotted as a function of t^2 at two different temperatures for (a) $Sr_2Cu(PO_4)_2$, (b) $Ba_2Cu(PO_4)_2$, and (c) $BaCuP_2O_7$. The solid lines show the fitting to a Gaussian function [Eq. (4)]. In the insets, $1/T_{2G}$ is plotted as a function of temperature T.

4. Spin-spin relaxation rate $1/T_{2G}$

Spin-spin relaxation was measured at $H \simeq 4$ kG, where the line is sufficiently narrow. The spin-spin relaxation was found to have a Gaussian behavior, and the rate $(1/T_{2G})$ was obtained by monitoring the decay of the transverse magnetization after a $\pi/2-t-\pi$ pulse sequence, as a function of the pulse separation time t, and fitting to the following equation:

$$M(2t) = M_0 \exp\left[-2\left(\frac{t}{T_{2G}}\right)^2\right] + C \qquad (4)$$

As shown in the inset of Fig. 7, the spin-spin relaxation rate $1/T_{2G}$ for all the samples is nearly temperature independent. $BaCuP_2O_7$ is the only compound that exhibits a significantly enhanced spin-spin relaxation rate $1/T_{2G}$ at the lowest temperature compared to elevated temperatures. This increase of $1/T_{2G}$ in $BaCuP_2O_7$ is most likely related to LRO.

IV. DISCUSSION

A. NMR shift

The general variation of the shift with temperature follows the expected behavior of an $S=1/2$ HAF chain, as seen in Sec. III. A steep decrease in $K(T)$ was observed below $k_BT/J \simeq 0.003$ for $Sr_2Cu(PO_4)_2$, $k_BT/J \simeq 0.0033$ for $Ba_2Cu(PO_4)_2$, and $k_BT/J \simeq 0.01$ for $BaCuP_2O_7$.[27] This decrease of K is clearly much more than the logarithmic decrease with an infinite slope at zero temperature, expected from theory (see solid line in Fig. 3). In $Sr_2Cu(PO_4)_2$, $Ba_2Cu(PO_4)_2$, and $BaCuP_2O_7$ (from Fig. 3), the extrapolated shifts at zero temperature were found to be 400, 590, and 580 ppm, respectively. The theoretically expected values, derived from the $T=0$ susceptibility[28] and using the relevant A and K_0, are 544, 740, and 738 ppm, respectively, for $Sr_2Cu(PO_4)_2$, $Ba_2Cu(PO_4)_2$, and $BaCuP_2O_7$. Among the various causes for this deviation, one might be the onset of spin-Peierls order. In such a case, the spin susceptibility (and, therefore, the spin shift) should vanish at $T=0$. However, our extrapolated $T=0$ shifts are much more than the chemical shifts K_0 and there is no exponential decrease of $1/T_1(T)$ toward low temperatures. Another possibility is the onset of three-dimensional (3D) LRO. In this case, a divergence should have been seen in the temperature dependencies of the spin-lattice relaxation rate $1/T_1$ as well as in the spin-spin relaxation rate $1/T_{2G}$. Although this is the case for $BaCuP_2O_7$, only a small increase of the relaxation rates is observed for $Sr_2Cu(PO_4)_2$ and $Ba_2Cu(PO_4)_2$. A clear effect is observed in the temperature dependencies of $K(T)$, $1/T_1$, $1/T_2$, and line shape for $BaCuP_2O_7$ at 0.85 K. This establishes the onset of LRO at 0.85 K in $BaCuP_2O_7$. However, in the case of $Sr_2Cu(PO_4)_2$ and $Ba_2Cu(PO_4)_2$, while a clear anomaly is seen in $K(T)$ at low-temperature, only a weak anomaly is seen in $1/T_1(T)$ and no significant changes were observed either in the low-temperature spectra or in $1/T_2(T)$. In summary, the presence or absence of LRO at low-temperatures in $Sr_2Cu(PO_4)_2$ and $Ba_2Cu(PO_4)_2$ cannot be unambiguously established.

B. Low-temperature NMR spectra for $BaCuP_2O_7$

From field-theory and Monte Carlo calculations, Eggert and Affleck[29] found that in case of half-integer spin chains, the local susceptibility near an open end of a finite chain has a large alternating component. This component appears in the form of staggered magnetization near chain ends, under the influence of an uniform field. This staggered moment has a maximum at a finite distance from the end and increases as $1/T$ with decreasing temperature. Analytical expression for the spin susceptibility $\chi(l)$ at site l were obtained which consist of the uniform (χ_u) and alternating (χ_{alt}) parts[29] $\chi(l) = \chi_u(l) + (-1)^l \chi_{alt}(l)$, where the uniform part is nearly constant and the alternating part is given by

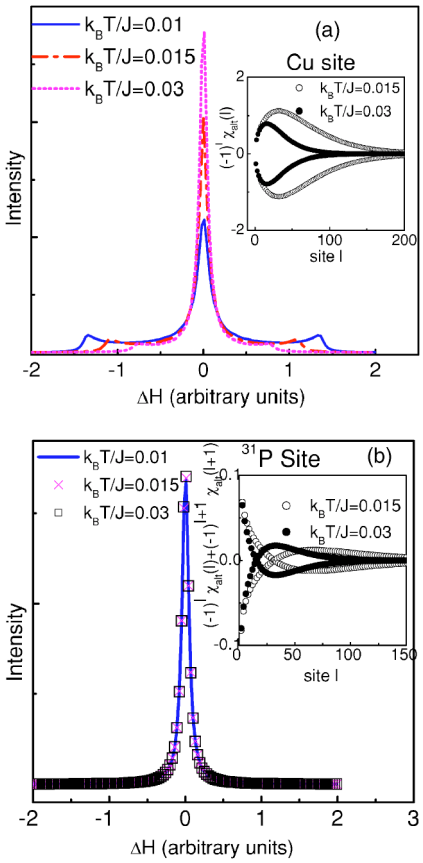

FIG. 8. Distribution function $g(x)$ which represents the NMR spectrum is plotted for (a) Cu site and (b) P site. In the insets of (a) and (b), $(-1)^l\chi_{\rm alt}(l)$ and $(-1)^l\chi_{\rm alt}(l)+(-1)^{l+1}\chi_{\rm alt}(l+1)$, respectively, are plotted as a function of the site index l from the chain end at two different temperatures.

$$\chi_{alt}(l) = \frac{aJ}{v}\frac{l}{\sqrt{(v/\pi T)\sinh(2\pi Tl/v)}} \tag{5}$$

where $v=\pi J/2$ is the spin-wave velocity. The NMR spectrum represents the distribution function of NMR shift, which is equivalent to χ_{alt}, and has the form $g(x)=\Sigma_l f[x-(-1)^l\chi_{alt}(l)]$, where f takes the form of a Lorentzian. This expression is valid for in-chain Cu^{2+} site. In our compounds, ^{31}P is the probe nucleus, which is sensitive to two nearest neighbor Cu^{2+} ions belonging to one chain. ^{31}P NMR line shape is then given by $g(x)=\Sigma_l f[x-\{(-1)^l\chi_{alt}(l)+(-1)^{l+1}\chi_{alt}(l+1)\}]$. Fig. 8 shows the simulated spectra for both Cu and P sites choosing f to be a Lorentzian with width 0.05.

For $k_BT=J/33$, at Cu site, χ_{alt} has a maximum at $l=0.48J/T$, which results in features in the spectra on either side of the central line. With increasing temperature these features on either side of the central peak disappear and $\sqrt{T}(\Delta H/2H_0)$ (where ΔH is the width at the background and H_0 is the field at the central peak) remain constant with temperature. This has been seen by Takigawa *et al.*[30] in ^{63}Cu NMR spectra of Sr_2CuO_3. However, the static effects of the staggered magnetization at the ^{31}P site in our compounds are expected to be much weaker [Fig. 8(b)] because of the near cancellation of the magnetization from the neighboring Cu sites.

Our low-temperature spectra for $Sr_2Cu(PO_4)_2$ and $Ba_2Cu(PO_4)_2$ show a single spectral line without any shoulders on either sides of the central peak. This is in agreement with our expectations that we are not sensitive to chain-end effects in ^{31}P NMR spectra of these compounds.

In low-field NMR on $BaCuP_2O_7$, a sudden increase of linewidth was observed below 0.85 K along with the appearance of two shoulderlike features located symmetrically on either side of the central peak [Fig. 5(d)]. If these shoulderlike features come from the staggered magnetization of chain ends, then, as discussed above, $\sqrt{T}(\Delta H/2H_0)$ should be temperature independent with the shoulders moving outward at lower temperatures. But in $BaCuP_2O_7$ the shoulder positions are temperature independent, suggesting that those features are not chain-end effects. Furthermore, in case of a structural phase transition, symmetrically located features that become more intense as temperature is lowered are not expected. Even for the case of conventional LRO, a large shift of the NMR line associated with a large magnetic field at the nuclear site because of the static electronic magnetization might be expected. The effect on the line shape seen here must stem from a magnetic transition possibly with exotic spin-order. In case of a transition to incommensurate (IC) order, a multipeak NMR spectrum is expected.[31] A recent example of this is $LiCu_2O_2$.[32] The general shape of our NMR spectrum appears to be similar to that in case of a two-dimensional phase modulation (in the plane-wave limit) of the magnetization. The frequency-dependent line shape in such a case is given by

$$f(\nu) = \frac{1}{(2\pi)^2}\int \frac{d\phi}{\sqrt{D_1^2-(\Delta\nu - D_2\cos\phi)^2}}, \tag{6}$$

where $\Delta\nu=\nu-\nu_0$ (ν_0 is the central peak position) and the integration extends over the region $|(\Delta\nu-D_2\cos\phi)/D_1|\leqslant 1$. A comparison to our spectra in Fig. 5(d) indicates that the qualitative shape near the shoulders and the singularities is reasonably well reproduced by Eq. (6) with $D_2=-0.286$ MHz, $D_1=-0.088$ MHz, and $\nu_0=6.71$ MHz. In Fig. 5(d), the x axis is taken in field units (which is obtained by multiplying the frequency by $\gamma/2\pi$) to compare to our experimental spectra. However, the persistence of the central line down to the lowest temperatures in our spectra suggests that there are regions that experience no significant change of the local field. Additionally, the shoulder and the singularity features have been found to shift with temperature for other compounds where IC order is found.[32] In $BaCuP_2O_7$, from 30 to 700 mK, the shoulder and the singularity positions remain nearly unchanged and as does the central line position. In view of this, a clear answer as to the nature of spin-order below 0.85 K in $BaCuP_2O_7$ is lacking. Although in other compounds the IC order is lattice driven, in the case of $BaCuP_2O_7$ it might be driven by a frustrating interchain interaction.

C. Wave vector q and temperature T dependence of $1/T_1$

In order to study the microscopic behavior of 1D HAF systems, it is useful to measure the temperature dependence of the spin-lattice relaxation rate, which yields information on the imaginary part of the dynamic susceptibility $\chi(\mathbf{q},\omega)$. The spin-lattice relaxation rate, in general, is affected by both uniform $(q=0)$ and staggered spin fluctuations $(q=\pm\pi/a)$. The uniform component leads to $1/T_1 \propto T$, while the staggered component gives $1/T_1=$constant.[7] At the ^{31}P sites, q dependence of $1/T_1$ can be expressed in terms of form factors as

$$1/T_1 \propto \sum_q [A^2 \cos^2(qx)]\mathrm{Im}\,\chi(q,\omega). \tag{7}$$

We are probing on the ^{31}P nucleus, which is linked to the Cu spins via oxygen atoms as shown in Fig. 1. Since ^{31}P is symmetrically located between the Cu ions, the antiferromagnetic fluctuations are filtered at the ^{31}P site, provided the two hyperfine couplings are equal. However, contributions just slightly differing from $q=\pi/a$ are apparently strong enough and/or the two hyperfine couplings are unequal and result in a qualitative behavior expected when relaxation is dominated by fluctuations of the staggered susceptibility.

If one were to ignore the geometrical form factor completely, the relaxation rate due to staggered fluctuations can be calculated following the prescription of Barzykin.[16] He obtained the normalized dimensionless NMR spin-lattice relaxation rate at low-temperature $(1/T_1)_{\mathrm{norm}}=\hbar J/(A_{th}^2 T_1) \approx 0.3$, where A_{th} is A $(2h\gamma/(2\pi))$. Assuming the fluctuations to be correlated, $1/T_1$ can be written as $1/T_1=0.3A^2/(\hbar J)$. Using this expression, $(1/T_1)$ at the ^{31}P site was calculated to be about 44 s^{-1}, 80 s^{-1}, and 47 s^{-1}, whereas our experimental values are 15 s^{-1}, 20 s^{-1}, and 25 s^{-1}, for $Sr_2Cu(PO_4)_2$, $Ba_2Cu(PO_4)_2$, and $BaCuP_2O_7$, respectively, in the 1 K$\leqslant T \leqslant$10 K range. The experimental values are clearly smaller than the theoretical ones because of the geometrical form factor. Furthermore, a logarithmic increase of $1/T_1$ is expected at low temperatures following:[16]

$$(1/T_1)_{\mathrm{norm}} = 2D\sqrt{\ln\frac{\Lambda}{T}+\frac{1}{2}\ln\left(\ln\frac{\Lambda}{T}\right)}\left(1+O\left[\frac{1}{\ln^2\frac{\Lambda}{T}}\right]\right), \tag{8}$$

where $D=1/(2\pi)^{3/2}$, Λ is the cutoff parameter given by $2\sqrt{2\pi}e^{C+1}J$ and C ($\simeq$0.5772157) is Euler's constant. In Fig. 9, we have plotted $[(1/T_1)/(1/T_1)_{T=10\ K}]_{\mathrm{norm}}$ calculated from Eq. (8) and the experimental results of the spin-lattice relaxation rate $1/T_1$ for our compounds normalized by their values at 10 K, as a function of temperature. The qualitative temperature dependence of the experimental spin-lattice relaxation rate $1/T_1$ agrees reasonably well with theoretical calculations in the constant region but below 0.5 K, the experimental increase in $Sr_2Cu(PO_4)_2$ and $Ba_2Cu(PO_4)_2$ is somewhat more than the logarithmic increase expected theoretically. However, complementary measurements are needed to fully understand this issue.

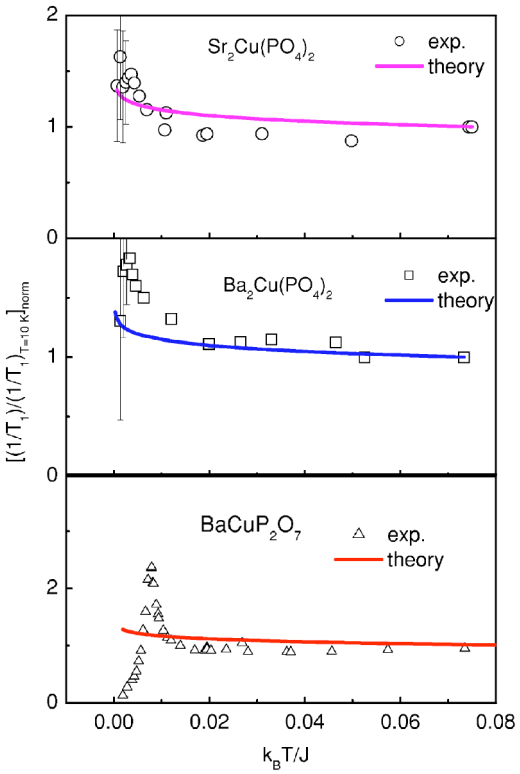

FIG. 9. Normalized experimental data (open symbols) as well as theoretical curves (solid lines) of $(1/T_1)_{\mathrm{norm}}$ are plotted vs k_BT/J for $Sr_2Cu(PO_4)_2$, $Ba_2Cu(PO_4)_2$, and $BaCuP_2O_7$ at low temperatures, 0.1 K$\leqslant T \leqslant$10 K. The data and the theoretical curves have been scaled to 1 at 10 K.

Another point to note is that the nearly temperature-independent spin-lattice relaxation rate sets in below $k_BT/J\sim0.12$ in our compounds. Sandvik[8] has performed quantum Monte Carlo simulations to calculate the temperature dependence of NMR $1/T_1$ for $S=1/2$ 1D HAF systems. This was done for variable values of the ratio R of the transferred hyperfine coupling to the on-site hyperfine coupling. From the results he concluded that in the limit of large and negative R, the nearly temperature-independent $1/T_1$ should be seen up to temperatures as high as $k_BT/J\sim0.5$, whereas for large and positive R, the constant behavior would be seen at much lower temperatures. In the present case, the on-site contribution (relevant for the ^{31}P nucleus) is clearly negligible since all the spin density should reside on the copper orbitals and the transferred hyperfine coupling was found to be positive. As a consequence, temperature-independent $1/T_1$ is seen only below $k_BT/J\sim0.12$. Above this temperature, the variation of $1/T_1$ is linear with T, though deviations from linearity are seen at temperatures higher than J/k_B [see Fig. 6(b)]. This change presumably signals an approach to temperature-independent behavior, which should be seen at high temperatures in the limit of noninteracting local moments. In fact one expects $1/(KT_1T)$ to be constant when the $q=0$ contribution dominates. From our data, $1/(KT_1T)$ is constant above 50 K for $BaCuP_2O_7$, while there is a weak temperature dependence for the cases of $Sr_2Cu(PO_4)_2$ $Ba_2Cu(PO_4)_2$ [see Fig. 6(c) inset]. This might be because of

some residual contribution from the staggered fluctuations. Since Sandvik's simulations are limited to $k_BT/J=1$, we are unable to compare our results for higher temperatures with theoretical simulations.

D. Spin-spin relaxation rate $1/T_2$

Following the treatment of Sachdev[7] and Barzykin,[16] spin-spin relaxation is expected to follow a Gaussian behavior with a temperature dependence given by $1/T_{2G} \propto 1/\sqrt{T}$. Further, the spinon mediated spin-spin relaxation rate can be calculated[16] as follows. The normalized spin-spin relaxation rate is given by $(\sqrt{T}/T_{2G})_{\text{norm}}=(k_BT/J)^{1/2}\hbar J/(A^2T_{2G})$. Dividing $(1/T_1)_{\text{norm}}$ by $(\sqrt{T}/T_{2G})_{\text{norm}}$ and equating it to 1.8 (the value obtained from Ref. 16) one finds that $1/T_{2G}=(44/1.8)(J/k_BT)^{1/2}$, $(80/1.8)(J/k_BT)^{1/2}$, and $(47/1.8)\times(J/k_BT)^{1/2}$, respectively for $Sr_2Cu(PO_4)_2$, $Ba_2Cu(PO_4)_2$, and $BaCuP_2O_7$. This leads to T_{2G} values 3.2, 1.8, and 3.6 ms in contrast to our experimental values 269, 255, and 207 μs, respectively, for $Sr_2Cu(PO_4)_2$, $Ba_2Cu(PO_4)_2$, and $BaCuP_2O_7$ at 1 K. These are almost three orders-of-magnitude smaller than the theoretically calculated values. Furthermore, our experimental spin-spin relaxation rates are temperature independent. Clearly, in the present case, spinon-mediated coupling does not contribute to spin-spin relaxation. On the other hand, an estimate of the nuclear dipole-dipole–mediated relaxation ($T_2 \sim r^3/(\gamma^2\hbar)$, where r is the dipole-dipole distance) would seem to explain the observed relaxation rates. This must be primarily because of the small exchange coupling in contrast to Sr_2CuO_3, where J is an order-of-magnitude larger and the spinon-mediated Gaussian spin-spin relaxation rate has been observed.

V. CONCLUSION

Our NMR and susceptibility measurements on $Sr_2Cu(PO_4)_2$, $Ba_2Cu(PO_4)_2$, and $BaCuP_2O_7$ show good agreement with the theory of 1D $S=1/2$ Heisenberg antiferromagnetic chains. NMR shift K as a function of temperature fitted well to the recent theoretical calculation by Johnston *et al.*,[6] and the exchange interaction J/k_B is estimated to be (165 ± 10) K, (151 ± 6) K, and (108 ± 2) K for $Sr_2Cu(PO_4)_2$, $Ba_2Cu(PO_4)_2$, and $BaCuP_2O_7$, respectively. We observed a steep decrease of the NMR shift $K(T)$ below $T\simeq 0.003\ J/k_B$, $0.0033\ J/k_B$, and $0.01\ J/k_B$ for $Sr_2Cu(PO_4)_2$, $Ba_2Cu(PO_4)_2$, and $BaCuP_2O_7$, respectively. Low-field ^{31}P NMR spectra of $BaCuP_2O_7$ shows sudden appearance of broad humps on either side of the central peak for $T<0.85$ K, indicating the onset of LRO. There are indications that the ordering might be incommensurate in nature. The spin-lattice relaxation rate $1/T_1$ was measured in a temperature range $0.02\ \text{K}\leqslant T\leqslant 300$ K. No clear indication of any kind of magnetic ordering was seen in $Sr_2Cu(PO_4)_2$ and $Ba_2Cu(PO_4)_2$ from the $1/T_1$ data, whereas a clear indication of magnetic ordering was observed at $T\approx 0.85$ K ($k_BT/J\approx 0.0079$) for $BaCuP_2O_7$. At low temperature, $1/T_1$ follows a nearly logarithmic increase for $T\leqslant 0.5$ K for $Sr_2Cu(PO_4)_2$ and $Ba_2Cu(PO_4)_2$, which is expected for a 1D $S=1/2$ HAF system. Though the transverse decays follow Gaussian behavior for all our samples, they result from dipole-dipole interaction rather than a spinon-mediated interaction. Our experimental evidence on these compounds strongly reflect their low-dimensional nature, making them one of the best 1D $S=1/2$ HAF systems that have been looked at thus far.

ACKNOWLEDGMENTS

We thank H.-A. Krug von Nidda for EPR measurements and H. Alloul for useful discussions. A.V.M. would like to thank the Alexander von Humboldt Foundation for financial support for the stay at Augsburg. This work was supported by the BMBF via VDI/EKM, FKZ 13N6917-A and by the Deutsche Forschungsgemeinschaft (DFG) through the Sonderforschungsbereich SFB 484 (Augsburg).

[1] F. D. M. Haldane, Phys. Rev. Lett. **50**, 1153 (1983).
[2] H. A. Bethe, Chem. Eng. Prog. **71**, 205 (1931).
[3] E. Lieb, T. D. Schultz, and D. C. Mattis, Ann. Phys. (N.Y.) **16**, 407 (1961).
[4] J. C. Bonner and M. E. Fisher, Phys. Rev. **135**, A640 (1964).
[5] S. Eggert, I. Affleck, and M. Takahashi, Phys. Rev. Lett. **73**, 332 (1994).
[6] D. C. Johnston, R. K. Kremer, M. Troyer, X. Wang, A. Klümper, S. L. Bud'ko, A. F. Panchula, and P. C. Canfield, Phys. Rev. B **61**, 9558 (2000).
[7] S. Sachdev, Phys. Rev. B **50**, 13006 (1994).
[8] A. W. Sandvik, Phys. Rev. B **52**, R9831 (1995).
[9] D. Hone, C. Scherer, and F. Borsa, Phys. Rev. B **9**, 965 (1974).
[10] P. M. Richards and F. Borsa, Solid State Commun. **15**, 135 (1974).
[11] J. Chakhalian, R. F. Kiefl, R. Miller, S. R. Dunsiger, G. Morris, S. Kreitzman, W. A. MacFarlane, J. Sonier, S. Eggert, I. Affleck, and I. Yamada, Physica B **326**, 422 (2003).
[12] N. Motoyama, H. Eisaki, S. Uchida, Phys. Rev. Lett. **76**, 3212 (1996).
[13] M. Takigawa, N. Motoyama, H. Eisaki, and S. Uchida, Phys. Rev. Lett. **76**, 4612 (1996).
[14] M. Takigawa, O. A. Starykh, A. W. Sandvik, and R. R. P. Singh, Phys. Rev. B **56**, 13681 (1997).
[15] K. R. Thurber, A. W. Hunt, T. Imai, and F. C. Chou, Phys. Rev. Lett. **87**, 247202 (2001).
[16] V. Barzykin, Phys. Rev. B **63**, 140412(R) (2001).
[17] A. A. Belik, A. P. Malakho, B. I. Lazoryak, and S. S. Khasanov, J. Solid State Chem. **163**, 121 (2002).
[18] K. M. S. Etheredge and Shiou-Jyh Hwu, Inorg. Chem. **35**, 1474 (1996).
[19] A. Moqine, A. Boukhari, and E. M. Holt, Acta Crystallogr., Sect. C: Cryst. Struct. Commun. **47**, 2294 (1991).
[20] A. A. Belik, M. Azuma, and M. Takano, J. Solid State Chem.

177, 883 (2004).

[21] A. A. Belik, M. Azuma, and M. Takano, J. Magn. Magn. Mater. **272–276**, 937 (2004).

[22] T. Ami, M. K. Crawford, R. L. Harlow, Z. R. Wang, D. C. Johnston, Q. Huang, and R. W. Erwin, Phys. Rev. B **51**, 5994 (1995).

[23] J. Das, A. V. Mahajan, J. Bobroff, H. Alloul, F. Alet, and E. S. Sorensen, Phys. Rev. B **69**, 144404 (2004).

[24] P. W. Selwood, *Magnetochemistry* (Interscience, New York, 1956).

[25] L. E. Drain, Proc. Phys. Soc. London **80**, 1380 (1962).

[26] A slightly higher $1/T_1$ at low-field is compatible with the results for Sr_2CuO_3, where it was explained by Takigawa[13] based on spin-diffusion.

[27] A similar decrease was observed in ^{17}O NMR shift of Sr_2CuO_3 below $k_BT/J \sim 0.015$.[15] In that case, it was suggested that the decrease was unrelated to magnetic ordering that took place at $k_BT/J \sim 0.002$ and might be a general feature of $S=1/2$ 1D HAF systems, so far not predicted theoretically.

[28] Using χ_{spin} $(T=0)$ from Ref. 2, $K(T=0)=K_0+[Ag^2\mu_B/k_B(J/k_B)]\times(1/\pi^2)$.

[29] S. Eggert and I. Affleck, Phys. Rev. Lett. **75**, 934 (1995).

[30] M. Takigawa, N. Motoyama, H. Eisaki, and S. Uchida, Phys. Rev. B **55**, 14129 (1997).

[31] R. Blinc, Phys. Rep. **79**, 333 (1981).

[32] A. A. Gippius, E. N. Morozova, A. S. Moskvin, A. V. Zalessky, A. A. Bush, M. Baenitz, H. Rosner, and S.-L. Drechsler, Phys. Rev. B **70**, 020406(R) (2004).